How to cite: *Angew. Chem. Int. Ed.* **2023,** *62,* e202215759
International Edition: doi.org/10.1002/anie.202215759
German Edition: doi.org/10.1002/ange.202215759

Molecular Computing

Computing Arithmetic Functions Using Immobilised Enzymatic Reaction Networks

*Nikita M. Ivanov[+], Mathieu G. Baltussen[+], Cristina Lía Fernández Regueiro[+], Max T. G. M. Derks, and Wilhelm T. S. Huck**

Abstract: Living systems use enzymatic reaction networks to process biochemical information and make decisions in response to external or internal stimuli. Herein, we present a modular and reusable platform for molecular information processing using enzymes immobilised in hydrogel beads and compartmentalised in a continuous stirred tank reactor. We demonstrate how this setup allows us to perform simple arithmetic operations, such as addition, subtraction and multiplication, using various concentrations of substrates or inhibitors as inputs and the production of a fluorescent molecule as the readout.

Introduction

Living systems process biochemical information through complex networks of coupled enzymatic reactions. These networks allow cells to maintain homeostasis and make decisions in response to external stimuli. In relaying information from cell surface receptors, the networks process this information and compute the appropriate responses based on the amplitude and duration of the input signals.[1–3] There is considerable interest in constructing synthetic analogues of such networks[4–6] to i) contribute to a more detailed understanding of the complexity of living systems, ii) enable the design of new materials with life-like properties,[7,8] such as autonomous sensing of their environment,[9–11] and iii) provide a route to molecular information processing systems, which could be an alternative to other types of computers.[12,13]

Various approaches to molecular information processing have been explored, including impressive examples of DNA-based computing.[4,14–17] While enzymatic networks lack the programmability or scalability that can be found in DNA networks, they include a much broader scope of chemical reactions, which could ultimately offer opportunities to couple computing properties of enzymatic networks with the measurement of metabolites or biomarkers in novel types of diagnostic devices. The use of enzymes in molecular computing studies has primarily focused on simple enzymatic systems generating Boolean logic networks.[5,18–22] In this study, we were inspired by theoretical work by Buisman et al.[23] outlining a general strategy to use small enzymatic reaction networks to perform simple arithmetic operations on steady-state concentrations. We envisage "molecular computers" built from enzymes as "hardware" and small molecule substrates and inhibitors as "software".

In particular, we used peptides containing a cleavable fluorogenic end group as well as specific cleavage sites for a number of different proteases as inputs to compute simple arithmetic functions. To avoid losing the enzyme "hardware" during information processing steps, we used a continuous stirred tank reactor (CSTR) containing enzymes immobilised on polyacrylamide hydrogel beads, as we reported recently (Figure 1a; for characterization of the enzyme-modified beads and details about the reactor, see the Supporting Information).[24] . We demonstrate that this "molecular information processing system" provides a robust platform for addition, subtraction and multiplication.

Results and Discussion

For this study we immobilised trypsin (Tr), chymotrypsin (Cr), elastase (Els) and aminopeptidase (Ap) on microfluidically prepared monodisperse polyacrylamide beads. Reactors loaded with enzyme beads retained constant activity for up to 60 days when stored at +4 °C (Supporting Information, S.3.4). Accurate estimation of the kinetic parameters of the enzymatic conversion is essential for the design of small networks carrying out arithmetic functions. We therefore built on our previously reported Bayesian analysis framework, where we showed how to combine multiple experimental datasets and prior information to obtain probabilistic kinetic parameters, automatically taking into account different experimental and epistemological uncertainties.[24]

In brief, two methods were used to obtain kinetic parameter estimates as shown in Figure 2: i) a previously reported[24] steady-state method, where the reactor loaded

[*] N. M. Ivanov,[+] M. G. Baltussen,[+] C. L. F. Regueiro,[+] M. T. G. M. Derks, Dr. Prof. W. T. S. Huck
Institute for Molecules and Materials, Radboud University
Heyendaalseweg 135, 6525AJ, Nijmegen (The Netherlands)
E-mail: w.huck@science.ru.nl

[+] co-first authors

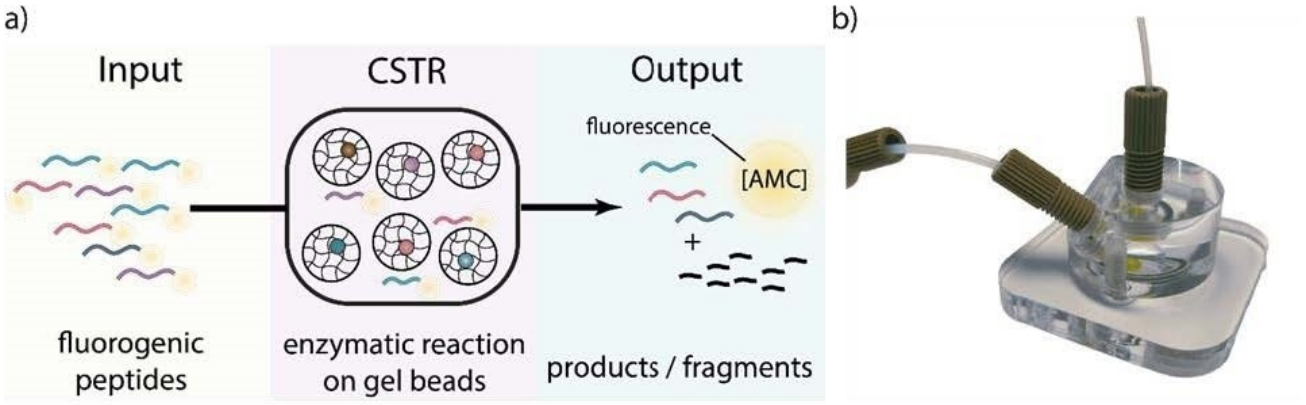

Figure 1. a) Hardware platform: enzymes immobilised on polyacrylamide beads are compartmentalized in a CSTR. Small molecules (peptides) are used as input for arithmetic operations that yield a fluorescent output, measured as fluorescence intensity of AMC. b) Photograph of the CSTR equipped with connectors. The inner reactor volume is 100 µL.

with enzyme beads is sequentially fed with increasing concentrations of the corresponding fluorogenic substrate, and at each concentration the steady-state conversion is measured (see Figure 2a,d); ii) a novel method applicable for the reactor packed with two enzymes based on dynamic inputs, where multiple substrate inputs were varied in a sawtooth-like pattern with different periodicities and amplitudes (see Figure 2g). In both methods the output is measured by determining the concentration of the fluorescent product, 7-amino-4-methylcoumarin (AMC), by passing the reactor outflow through a flow cell positioned in a spectrofluorimeter or by fluorimetry following fraction collection (details in Supporting Information, section S.1.b, S.3). Please note: enzymatic activity after immobilization is inevitably altered, but in this study it is essential to know the activity of enzyme-loaded beads. We therefore use Michaelis–Menten-type kinetic parameters that relate to the maximum activity of the reactor (i.e. $V_{max,reactor}$, $K_{M,reactor}$). This allows us to reproducibly obtain kinetic parameters for different batches of enzyme-loaded beads. These parameters are obtained by fitting the observed data to ordinary differential equations modified with appropriate flow-terms (Supporting Information section S.3.5). As shown in Figures 2b,c and 2e,f, both methods yield accurate estimates. We found that the dynamic input method results in more precise estimates at an order-of-magnitude shorter experimental timescales and reduced material cost but is more difficult to implement experimentally than the steady-state method. Furthermore, it requires some prior information on the kinetic parameter values. Generally, either or both methods can be employed, depending on the required estimate precisions and experimental circumstances.

With the "hardware" in place, we could explore the implementation of simple "molecular computation" modules by carrying out basic arithmetic operations. Specific topologies of catalytic networks can behave like arithmetic operators on steady-state concentrations. In our modules, (changes in) concentrations of small molecules are the inputs of the operations, and the outputs are the fluorescence intensity of AMC measured at steady-state. Unlike batch reactions, the reactions in flow proceed to a certain degree of conversion. The degree of conversion is dependent on the flow, and it is possible to regulate the reaction outputs by adjusting the flow rate (see Supporting Information section S.4.1.b,c).

Addition is the most basic arithmetic operation: it combines two or more quantities into a single quantity. Figure 3a depicts the networks used for accomplishing this operation: two sufficiently orthogonal enzymes, chymotrypsin and elastase, independently catalyse the production of the same fluorescent product by cleaving their specific fluorogenic substrates (S_{Cr} and S_{Els}, respectively), and the total AMC production is the sum of the two enzymatic reactions (see Supporting Information section S4.2 for derivation):

$$[AMC] = a[S_{Els}] + b[S_{Cr}], \quad (1)$$

where *a* and *b* are activity parameters for Els and Cr, respectively (see Supporting Information Table S.4 for values).

Figure 3b shows the experimental results for this system. The purple and pink columns show the AMC production from substrates S_{Els} and S_{Cr} added sequentially, whereas the green column shows AMC production using both substrates simultaneously. Clearly, in both cases the addition yields the same result. The box plot to the right of each column represents the prediction of the total AMC production according to the linear equation based on separately estimated kinetic parameters (see Supporting Information section S4.1). At higher S_{Els} concentrations, the observed AMC production starts to deviate from the linear addition model. This is not unexpected because at higher substrate concentrations we are no longer in the linear response regime of Michaelis–Menten kinetics, and these data show the limitations in functional range of the arithmetic operations we can perform. The reproducibility of the system was demonstrated by repeating the addition operation over

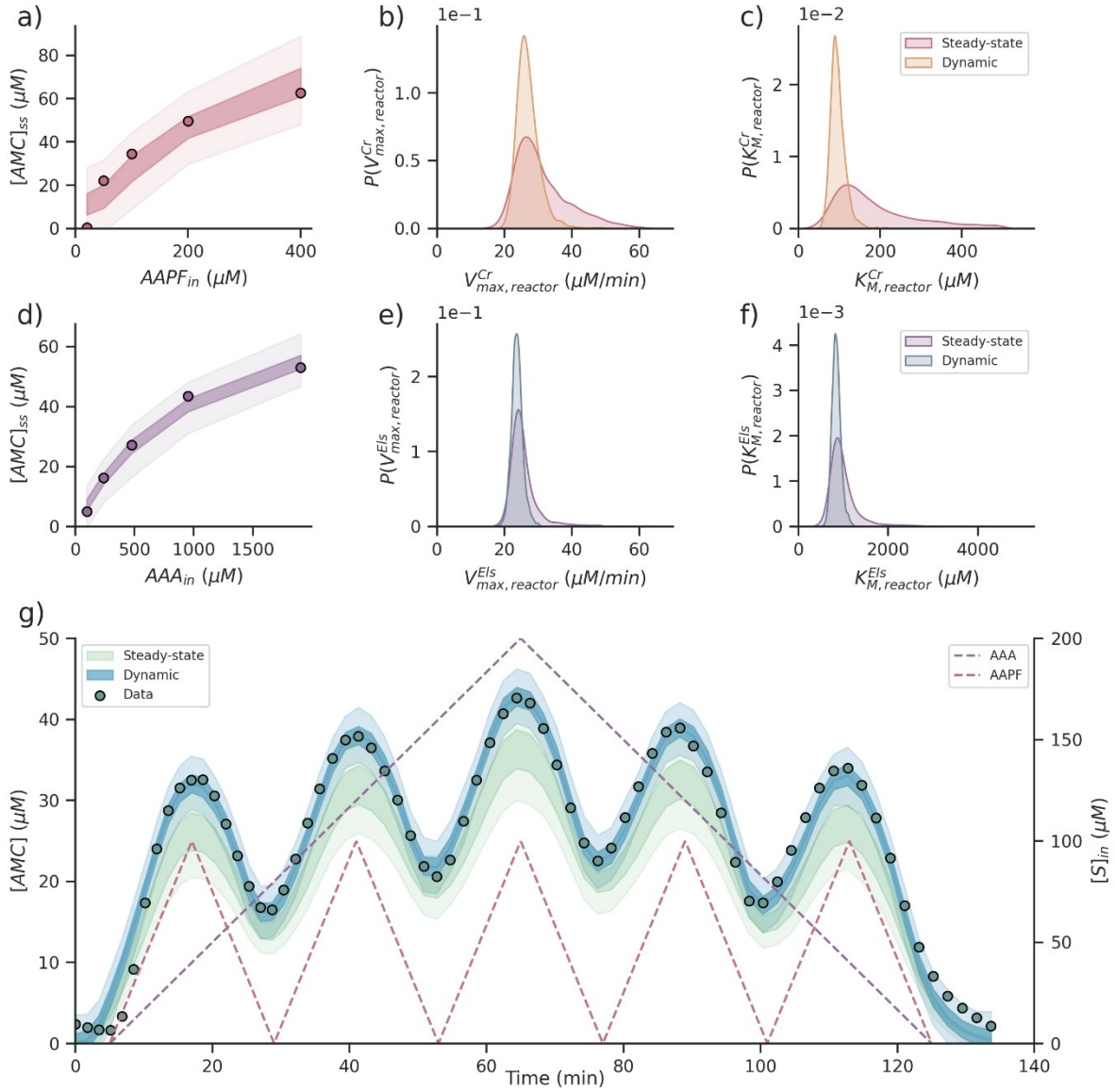

Figure 2. a) Shaded confidence intervals (CI) of Bayesian fits (95% and 50%) of steady-state experiment of cleavage of Suc-AAPF-AMC by chymotrypsin (Cr). b,c) Kinetic parameter estimates for Cr obtained from just the steady-state experiment, and improved by the dynamic input experiment. d) Shaded confidence intervals of Bayesian fits (95% and 50% of steady-state experiment of cleavage of Suc-AAA-AMC by elastase (Els)). e,f) Kinetic parameter estimates for Els obtained from just the steady-state experiment, and improved by the dynamic input experiment. g) Dynamic input experiment, showing the sawtooth pattern of both input substrates as dashed lines, as well as the predicted output from just the steady-state estimates (green, CI 95/50%), and the final inference of the observations (blue, CI 95/50%).

the course of a week using the same CSTR (more details in Supporting Information S4.2.c). Besides, it is possible to manipulate the parameters *a* and *b* from Equation (1) by changing the flow rate (Supporting Information section S.4.2.d), which effectively combines addition with multiplication by a factor.

Although addition might be straightforward in small networks, designing complex networks with more components is not trivial. The promiscuity of enzyme active sites, substrate competition, and possible side interactions between input or output molecules and the enzymes can significantly influence the final output of the system.[25–27] For example, a substrate saturating the active site of one enzyme can globally affect the conversion of other substrates affecting the final response of the system.[22] Cross-reactivity can be identified within the overall dynamics of complete experimental sets, as they represent the deviation from the simple model. Figure 3c describes the three enzyme-three substrate system and the outputs of this system. In Figure 3d, the pink bar depicts the theoretical sum of AMC concentration produced by each enzymatic reaction, not considering possible cross-reactivity. The green column represents the experimentally obtained AMC concentration using three enzymes and simultaneously flowing different concentrations of the three substrates. The experimental output (green column)

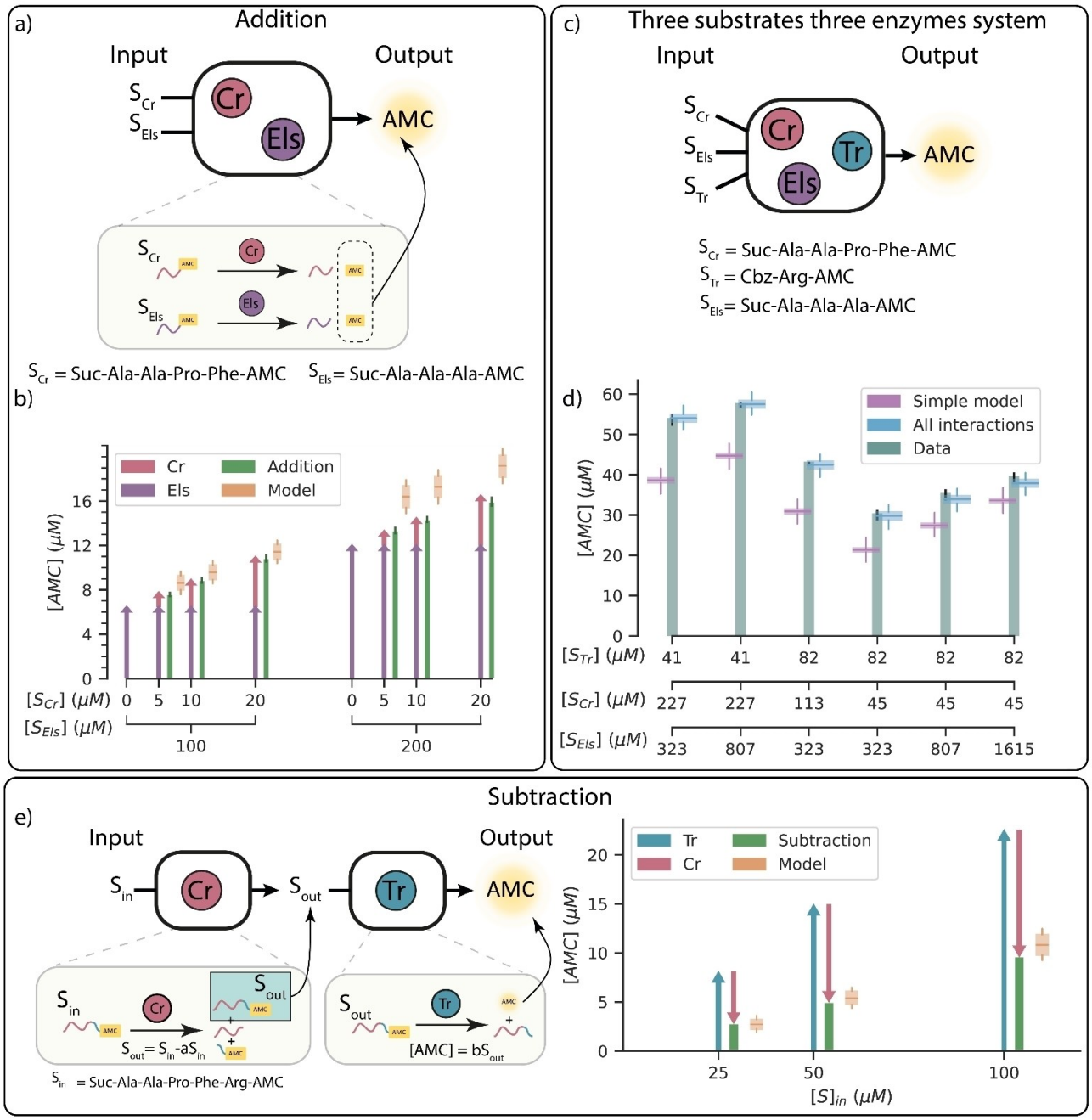

Figure 3. a) Addition network: chymotrypsin (Cr) and elastase (Els) independently catalyse the production of AMC. b) Fluorescence intensities of AMC measured after adding substrates S_{Cr} (pink) or S_{Els} (purple) sequentially or simultaneously (green). The box plots show the expected value for addition based on the linear model. c) Diagram of a three substrate-three enzyme addition reactor. d) Production of AMC at six input combinations. Green columns show the experimental data for the AMC production. The pink and blue box plots show the predicted values using, respectively, a simple linear model or a full model including cross-interactions. e) Diagram of the subtraction motif and output response. The system comprises two reactors in series, the first one containing Cr beads and the second Tr beads. The graph shows in blue the production of AMC when S is fed only into the reactor with Tr beads. Pink columns show the decrease in AMC production when both reactors are used. The box plots correspond to the modelled AMC production.

does not match simple theoretical predictions (pink bar) based on the AMC production from individual enzymes. To address this problem, we need to consider other processes such as cross-reactivity. The kinetic constants for cross-inhibition by the various substrates, and cleavage of S_{Cr} by trypsin, could not be estimated directly. We therefore fitted kinetic parameters using a dataset containing two experiments of 27 different conditions (see Supporting Information section S.4.3 for substrate input concentrations used and fitting procedure). The obtained final estimates fit the output well, as shown in Figure 3d (blue boxes).

Further, we demonstrated a simple subtraction motif (Figure 3e) by exploiting the catalytic activity of trypsin and chymotrypsin towards substrate Suc-Ala-Ala-Pro-Phe-Arg-AMC (S_{in}). We used two concatenated reactors containing chymotrypsin and trypsin, respectively. Trypsin catalyses the release of AMC, whereas chymotrypsin cleaves the same peptide after phenylalanine, thereby producing non-fluorescent fragments. The R-AMC fragment cannot be cleaved by Tr beads, because of Tr being a strict endopeptidase. This leads to a decreased substrate concentration available for trypsin. The final AMC concentration can thus be calculated proportionally to the difference between the initial concentration of Sin and the reacted Sin after going through the first reactor, which depends on chymotrypsin activity (see Supporting Information, section S.4.4 for details):

$$[\mathrm{AMC}] = b[\mathrm{S}]_{in} - ab[\mathrm{S}]_{in}, \quad (2)$$

where *a* and *b* are activity parameters for Cr and Tr, respectively (see Supporting Information Table S.9 for values).

Figure 3f shows the experimental results of this system and a comparison with predictions made from the linear model in Equation (2), using previously estimated kinetic parameters. Interestingly, the substrate regime for which the subtraction operation is valid extends beyond the linear regime for both enzyme reactions individually, as the non-linear effects cancel out.

Multiplication can be performed when two catalysts subsequently participate in the output production.[23] The network depicted in Figure 4a shows two enzymatic concatenated identification operations taking place in the same reactor. Chymotrypsin, controlled by aprotinin, cleaves a peptide substrate (S) in the first reaction, yielding an intermediate peptide (I). In the second reaction, aminopeptidase (Ap), controlled by bestatin, consumes the intermediate peptide (I) to produce the fluorescence output (AMC). The overall fluorescence intensity represents the multiplication of the activities of both enzymes (controlled by the level of inhibitor concentration used). While aprotinin and bestatin act as reversible and competitive inhibitors of free Cr and Ap,[28,29] they were found to inhibit Cr and Ap beads with reversible and mixed, close to competitive mechanisms (see Supporting Information section S.4.5.b for kinetic details) without cross-inhibition. Notably, the highest enzyme activity is restricted by the minimum flow rate of the pumps. The lowest enzyme activity is restricted by non-complete inhibition: Even at high inhibitor concentrations, the activity is 0.6–0.8 from the activity without inhibitors.

Under the chosen conditions, the steady-state output concentration of AMC is dependent on the normalised enzyme activities as (see Supporting Information section S.4.5a for full details):

$$[\mathrm{AMC}]_{norm.} = \alpha(\mathrm{A})_{norm.} \times \beta(\mathrm{B})_{norm.} \quad (3)$$

$$\alpha(\mathrm{A}) \text{ or } \beta(\mathrm{B}) = \frac{\frac{k_{cat}[E]}{K_M + \frac{[Inh]}{K_{inh}}}}{\frac{k_{cat}[E]}{K_M + \frac{[Inh]}{K_{inh}}} + k_{flow}}. \quad (4)$$

The enzyme activities α and β are defined as functions of the input concentration of inhibitors (Inh) A, B [Eq. (4)] and are referenced to activity under standard

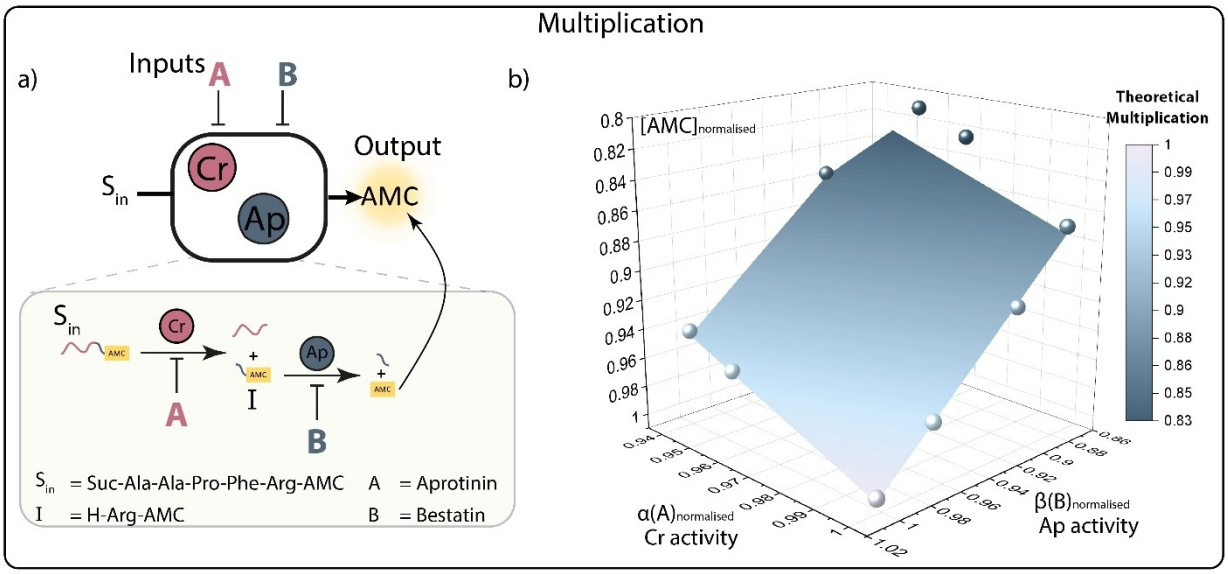

Figure 4. a) Multiplication motif. The reactor contains a mixture of Cr and Ap beads. The substrate (S_{in}) is fed into the reactor, where it first undergoes proteolytic cleavage by Cr, producing an intermediate peptide (I) that can then be cleaved by Ap, producing AMC fluorescence. Different combinations of inhibitor concentrations (bestatin and aprotinin) are used as inputs for multiplication as explained in the text. b) The graph shows AMC production in the multiplication topology when varying the enzymatic activity with different combinations of input (α(A) and β(B)). The spheres in the graph represent experimental data. The surface plot shows the theoretical AMC production obtained from multiplying the normalised enzyme activity values for each input combination.

conditions (see Supporting Information section S.4.5.a for more details). The graph in Figure 4b shows the normalised AMC concentrations (spheres) obtained from the system when varying the enzymatic activity (α and β), with different combinations of input (A and B). The surface plot shows the theoretical data obtained from multiplying the normalised values of enzyme activity for each input, which is in agreement with the experimental data.

Conclusion

We have demonstrated how enzymes, immobilized on hydrogel beads and compartmentalised in a CSTR, form a modular and reusable platform for molecular information processing. Building on previous work using Bayesian inference, we showed how dynamic inputs allow for more precise kinetic parameter estimations at reduced experimental timescales and material costs, and how the existence of cross-reactivity can be deduced from larger experimental datasets, both allowing for more precise design and implementation of enzymatic motifs with specific functionality. Using small molecules (peptide-based substrates and inhibitors) as input, we established the most fundamental arithmetic operations (addition, subtraction, multiplication) on steady-state concentrations of reagents. As shown theoretically,[23] a broader range of arithmetic functions may be available through catalytic networks; however, the kinetics of enzymatic reactions disfavours construction of certain units (e.g., square root can be computed by a network with a second-order reaction $2A \rightarrow X$, $v = k[A]^2$, but this rate law is not typical for enzymatic reactions). Finding sets of network topologies for a desired output function therefore remains an important challenge. As an alternative to implementing analogue functions, one could consider the construction of Boolean logic gates, with addition and multiplication forming equivalents of Boolean OR and AND gates, respectively.

We have presented a novel route to enzymatic systems that act as elements of computational analog circuits. By compartmentalising the "hardware", we can construct more complex systems, in which the small molecule "software" can be used to connect different modules. This approach will allow us to go beyond individual and simple motifs and even connect multiple reactors to implement more complex functions. We foresee potential future applications in diagnostic devices,[20] where enzymatic networks could perform a simple arithmetic operation on concentrations of molecules present in a biological sample, which would then be further translated into a final (possibly electronic) signal by Boolean operators.

Acknowledgements

We thank Arjan H. de Kleine and Jeroen van de Wiel for their help and work in the design and manufacturing of the CSTRs. This project has received funding from the European Research Council (ERC) under the European Union's Horizon 2020 research and innovation programme (ERC Adv. Grant Life-Inspired, grant agreement No. 833466) and the Dutch Ministry of Education, Culture and Science (Gravity program 024.001.035).

Conflict of Interest

The authors declare no conflict of interest.

Data Availability Statement

The data that support the findings of this study are available in the supplementary material of this article.

Keywords: Analog Computing · Enzymatic Reaction Networks · Enzyme Immobilisation · Molecular Computing · Molecular Information Processing

[1] D. Bray, *Nature* **1995**, *376*, 307–312.
[2] B. N. Kholodenko, *Nat. Rev. Mol. Cell Biol.* **2006**, *7*, 165–176.
[3] J. E. Ferrell, *Cell Syst.* **2016**, *2*, 62–67.
[4] A. P. Liu, E. A. Appel, P. D. Ashby, B. M. Baker, E. Franco, L. Gu, K. Haynes, N. S. Joshi, A. M. Kloxin, P. H. J. Kouwer, J. Mittal, L. Morsut, V. Noireaux, S. Parekh, R. Schulman, S. K. Y. Tang, M. T. Valentine, S. L. Vega, W. Weber, N. Stephanopoulos, O. Chaudhuri, *Nat. Mater.* **2022**, *21*, 390–397.
[5] R. Baron, O. Lioubashevski, E. Katz, T. Niazov, I. Willner, *Angew. Chem. Int. Ed.* **2006**, *45*, 1572–1576; *Angew. Chem.* **2006**, *118*, 1602–1606.
[6] A. Walther, *Adv. Mater.* **2020**, *32*, 1905111.
[7] S. N. Semenov, A. S. Y. Wong, R. M. Van Der Made, S. G. J. Postma, J. Groen, H. W. H. Van Roekel, T. F. A. De Greef, W. T. S. Huck, *Nat. Chem.* **2015**, *7*, 160–165.
[8] M. M. Lerch, A. Grinthal, J. Aizenberg, *Adv. Mater.* **2020**, *32*, 1905554.
[9] P. A. Korevaar, C. N. Kaplan, A. Grinthal, R. M. Rust, J. Aizenberg, *Nat. Commun.* **2020**, *11*, 386.
[10] L. Heinen, T. Heuser, A. Steinschulte, A. Walther, *Nano Lett.* **2017**, *17*, 4989–4995.
[11] S. G. J. Postma, I. N. Vialshin, C. Y. Gerritsen, M. Bao, W. T. S. Huck, *Angew. Chem.* **2017**, *129*, 1820–1824.
[12] A. Arkin, J. Ross, *Biophys. J.* **1994**, *67*, 560–578.
[13] Y. Benenson, *Nat. Rev. Genet.* **2012**, *13*, 455–468.
[14] L. Qian, E. Winfree, J. Bruck, *Nature* **2011**, *475*, 368–372.
[15] L. Ceze, J. Nivala, K. Strauss, *Nat. Rev. Genet.* **2019**, *20*, 456–466.
[16] A. M. Mohammed, P. Šulc, J. Zenk, R. Schulman, *Nat. Nanotechnol.* **2017**, *12*, 312–316.
[17] S. Okumura, G. Gines, A. Baccouche, R. Deteix, T. Fujii, Y. Rondelez, A. J. Genot, *Nature* **2022**, *610*, 496–501.
[18] E. Katz, V. Privman, *Chem. Soc. Rev.* **2010**, *39*, 1835–1857.
[19] E. Katz, *ChemPhysChem* **2019**, *20*, 9–22.
[20] E. Katz, *Enzyme-Based Computing Systems*, Wiley-VCH, Weinheim, **2017**, pp. 9–75, 211–219, 235–276.
[21] N. Wagner, G. Ashkenasy, *Chem. Eur. J.* **2009**, *15*, 1765–1775.
[22] A. J. Genot, T. Fujii, Y. Rondelez, *Phys. Rev. Lett.* **2012**, *109*, 208102.
[23] H. J. Buisman, H. M. M. ten Eikelder, P. A. J. Hilbers, A. M. L. Liekens, *Artif. Life* **2009**, *15*, 5–19.

[24] M. G. Baltussen, J. van de Wiel, C. L. Fernández Regueiro, M. Jakštaitė, W. T. S. Huck, *Anal. Chem.* **2022**, *94*, 7311–7318.
[25] Y. Zhang, S. Tsitkov, H. Hess, *Nat. Catal.* **2018**, *1*, 276–281.
[26] Y. Pan, W. Qiu, Q. Li, S. Zhu, C. Lin, W. Zeng, X. Xiong, X. Y. Liu, Y. Lin, *ChemCatChem* **2019**, *11*, 1878–1883.
[27] S. N. Semenov, A. J. Markvoort, W. B. L. Gevers, A. Piruska, T. F. A. De Greef, W. T. S. Huck, *Biophys. J.* **2013**, *105*, 1057–1066.
[28] H. Suda, T. Aoyagi, T. Takeuchi, H. Umezawa, *Arch. Biochem. Biophys.* **1976**, *177*, 196–200.
[29] D. Belorgey, S. Dirrig, M. Amouric, C. Figarella, J. G. Bieth, *Biochem. J.* **1996**, *313*, 555–560.

Manuscript received: October 26, 2022
Accepted manuscript online: December 23, 2022
Version of record online: January 12, 2023